

Received March 11, 2020, accepted March 25, 2020, date of publication March 30, 2020, date of current version April 15, 2020.

Digital Object Identifier 10.1109/ACCESS.2020.2984021

A Quadratic Polynomial Receiving Scheme for Sinusoidal Signals Enhanced by Stochastic Resonance Under Color Noise

HOUDE QUAN¹, GUANGKAI LIU¹, HUIXIAN SUN^{1,2},
XIAOHAN WANG³, AND XIAOLU ZHANG⁴

¹Department of Electronic and Optical Engineering, Army Engineering University, Shijiazhuang 050003, China

²National Key Laboratory of Science and Technology on Communications, University of Electronic Science and Technology of China, Chengdu 611731, China

³Center of Equipment Training Simulation, Army Engineering University, Shijiazhuang 050003, China

⁴The troop of 95010, Shantou 515000, China

Corresponding author: Guangkai Liu (dreamer_gk@163.com)

This work was supported in part by the National Natural Science Foundation of China under Grant 61531009 and Grant 61471108, and in part by The National Major Projects of China under Grant 2016ZX03001009.

ABSTRACT In this paper, a receiving scheme for intermediate frequency (IF) signals enhanced by stochastic resonance (SR) is proposed. The proposed scheme mitigates the reception failure of these signals, which can occur in radio and communication systems under extremely low signal-to-noise ratio (SNR). The SR mechanism for enhancing sinusoidal signals is analyzed. An analytic solution with time parameters of the Fokker-Planck Equation (FPE) is obtained by introducing the decision time from the non-autonomous FPE into an autonomous one. A quadratic polynomial receiving structure for sinusoidal signals enhanced by SR is proposed by comparing the characteristics of energy detection and matched filter detection. And the polynomial coefficients of the quadratic system are obtained by maximizing the deflection. Based on the idea of “the average of N samples” and the assumption of Gaussian distribution approximation under the law of large numbers, a quadratic polynomial receiving scheme for sinusoidal signals enhanced by SR is proposed. The conclusions are as below: 1) when the noise intensity is constant, the smaller the correlation time, the bigger the local SNR around the IF frequency due to the better performance of the low-pass filter; 2) The error bit ratio of the quadratic polynomial receiver is less than 1×10^{-2} when $N = 20$ and the SNR is above -14 dB, which can be applied to the military emergency communication under extremely low SNR. Experiment verifies the theory.

INDEX TERMS Stochastic resonance, the reception of sinusoidal signal, a quadratic polynomial receiving scheme, the Fokker-Planck Equation, deflection.

I. INTRODUCTION

The conventional intermediate frequency (IF) signal widely used in super-heterodyne receiver in radio and communication systems are the typically sinusoidal. And the IF signal can be effectively detected and received when the signal-to-noise ratio (SNR) is higher than 0dB. What is more, in the traditional communication systems, the SNR is usually between 0 dB and 20 dB. However, the Dual-Sequence-Frequency-Hopping (DSFH) communication mode is mainly used in the military emergency communication under very low SNR [1]–[3], which is lower than -10 dB. Further region

The associate editor coordinating the review of this manuscript and approving it for publication was Prakasam Periasamy¹.

of low SNR varies with different systems [4]. And the super-heterodyne receiving scheme is used in DSFH. So successfully detecting and receiving the IF signal under strong interference or at an SNR much smaller than 0 dB is the main research direction in DSFH system and other military emergency communication. And the IF signal received by the super-heterodyne receiver is the sinusoidal wave, which is a typical input signal of the stochastic resonance (SR).

SR is a nonlinear physical phenomenon, which goes against the common concept that the presence of noise is always harmful for signal detection. In fact, noise can enhance the detection performance of nonlinear SR systems when the signal, noise and the SR parameters are matched. Benzi firstly proposes the SR phenomenon in the research

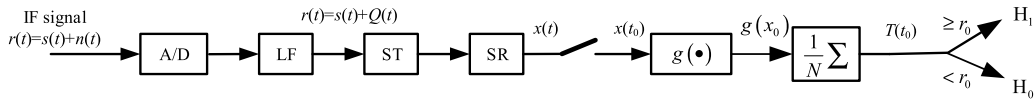


FIGURE 1. A generalized receiver of the IF signal processed by SR.

of the earth glacier [5]. And then SR is demonstrated in the fields of physics, biology and electronics [6]–[10]. Lots of researchers apply it to the signal detection when the signal intensity is lower than the decision threshold [11], [12]. V. Galdi *et al.* studies the optimal receiver by the maximum likelihood detection under the Gaussian white noise. The problem of combining SR with signal detection is primarily addressed by test statistics such as mean, zero-crossing and non-coherent detection [13]. However color noise is the most common type of noise in practical scenarios, receiving an IF signal under color noise is a problem of high practical significance. And the IF signal received by the super-heterodyne receiver, submerged in noise when the SNR is far below 0dB, will be filtered by the low-pass filter. Then the noise turns into color. And some researchers study the SR under color noise. Base on this practical engineering case, M.A. Fuentes and Raul Toral study the effects of non-Gaussian noises on SR, using the path-integral method and obtaining the periodic solution of the Fokker-Planck Equation (FPE) [14]. For further expanding the application, Hao Chen *et al.* analyze the signal detection enhanced by SR, and raise the generalized receiving structure by the detection probability and false probability under different criteria [15], [16]. Kang *et al.* analyze the optimal threshold of signal detection enhanced by SR, via maxing the SNR under the α stable noise [17]. Zhang *et al.* study the effect on logical SR bringing by color noise, and conclude that the signal detection of logical SR can be raised by adding the period signal under color noise [18]. Xia *et al.* apply the SR to the prognostics and health management (PHM) field [19] and introduce the review in PHM [20]. Duan *et al.* apply the SR to the binary signal transmission in nonlinear sensors, and obtain that the noise can play a constructive role in binary signal transmission [21]. Liu *et al.* apply the SR to the classification of hyperspectral image, and conclude that this method can be used to the information exploration of the shadow areas with small samples and different targets [22].

For the detection and reception of the IF signal processed by SR, the bi-stable SR mechanism of sinusoidal wave affected by color noise is analyzed. By assuming that the SR transitive motion of electronic particles is instantaneous and introducing the decision time, the non-autonomous FPE is transacted to an autonomous one. Then the periodic steady-state solution of FPE with the decision time parameter is obtained. A quadratic polynomial receiving scheme for sinusoidal signals enhanced by SR under color noise is raised compared with the energy receiver and the matching filtering receiver. In order to reduce the error, the idea of “the average of N samples” is introduced. And through the central limit theorem, the problem is transformed into a

typical hypothesis test problem under Gaussian noise. Then the receiving scheme is proposed and the theoretical results are verified by simulation. The paper is organized as follows: In Section 2, we investigate system model. Section 3 is devoted to the SR enhanced mechanism of the sinusoidal signal detection, and the probability density function (PDF) of the SR output. In section 4, the quadratic polynomial receiving scheme and the performance are analyzed. Section 5 discusses the simulation results. And the last section draws some conclusions.

II. SYSTEM MODEL

The IF signal receiving structure enhanced by SR can be described as Fig. 1.

The IF signal received by the super-heterodyne receiver is submerged in the noise leading that the SNR is much less than 0dB. Then the IF signal is over sampled by the A/D converter like 200 times. And due to oversampling, the IF signal is located in the low frequency region of the entire band. Therefore the received signal $r(t)$ can be filtered by a low-pass filter. The noise $Q(t)$ processed by the filter is color and non-Gaussian, and its spectrum can be modeled as a Lorentz form. What is more, in order to meet the needs of SR parameters, $r(t)$ has to be scale transacted. Then be processed by SR. For symbol reception, we only focus on the signal value $x(t_0)$ at the decision time t_0 . In order to improve the receptive performance, the receiving structure $g(\cdot)$ is raised to fit the waveform of $x(t_0)$ at the decision time t_0 . And to reduce the error further, the receiving structure of “the average of N samples” is proposed. The test statistic at the decision time t_0 is then compared with the threshold r_0 , which is above corresponding to 1 and below corresponding to 0.

The noise $Q(t)$ processed by low-pass filter becomes color and non-Gaussian, and its corresponding correlation function

$$\langle Q(t) Q(t') \rangle = \frac{D}{\tau} \exp\left(-\frac{|t-t'|}{\tau}\right) \quad (1)$$

where τ is the correlation time, D is the noise intensity. And its spectrum has a Lorentzian form like $S(\omega) = \frac{2D}{1+\tau^2\omega^2}$.

Next we will analyze the SR mechanism of the sinusoidal signal detection under color noise.

III. THE SR ENHANCED MECHANISM OF THE SINUSOIDAL SIGNAL DETECTION

A. THE SR DESCRIPTION OF SINUSOIDAL WAVE

The overdamped bi-stable SR enforced by sinusoidal wave $A \cos(\omega_0 t + \phi)$ and color noise $Q(t)$ can be depicted as

follows

$$\frac{dx}{dt} = ax - bx^3 + A \cos(\omega_0 t + \varphi) + Q(t) \quad (2)$$

where a and b are the SR parameters, $A \cos(\omega_0 t + \varphi)$ is the periodic signal.

With the reason that SR unite can only settle the small signal with small frequency and amplitude, so the IF signal with large frequency and amplitude needs to be transacted to small one, which is done by the ST unite. Therefore we introduce the variable substitution [23] $z = x\sqrt{\frac{b}{a}}$, $\tau = at$, the equation (2) can be transacted to

$$\frac{dz}{d\tau} = z - z^3 + \sqrt{\frac{b}{a^3}}A \cos\left(\frac{\omega_0}{a}\tau + \varphi\right) + \sqrt{\frac{2Db}{a^2}}Q(\tau) \quad (3)$$

So, the frequency scale transacted equation is $\frac{\omega_0}{a} = 2\pi f$, where the frequency is transacted to the $1/a$ times of the original. The amplitude scale transacted equation is $A_0 = \sqrt{\frac{b}{a^3}}A$. When a is large enough and b is small enough, the large IF signal can be transacted to small one after ST. At the same time, the noise intensity becomes $D_0 = \sqrt{\frac{2Db}{a^2}}$. In order to accord with the habit of representation of variables, equation (3) is rewritten as

$$\frac{dx}{dt} = x - x^3 + \sqrt{\frac{b}{a^3}}A \cos\left(\frac{\omega_0}{a}t + \varphi\right) + \sqrt{\frac{2Db}{a^2}}Q(t) \quad (4)$$

Due to the correlation time of $Q(t)$, the equation (4) is not Markov process which can not be derived to a FPE by the method of transition moment and Kramer-Moyal expansion. So we can extend it into two dimensional space, which can be described by Markov process as follows

$$\begin{cases} \frac{dx}{dt} = C(x) + \sqrt{\frac{2Db}{a^2}}y \\ \frac{dy}{dt} = -\frac{1}{\tau}y + \frac{1}{\tau}\Gamma(t) \end{cases} \quad (5)$$

where $C(x) = x - x^3 + \sqrt{\frac{b}{a^3}}A \cos\left(\frac{\omega_0}{a}t + \varphi\right)$, $\Gamma(t)$ is the Gaussian white noise with intensity of D .

Therefore using the method of transition moment and Kramer-Moyal expansion [24], the corresponding FPE of equation (5) can be described as

$$\begin{aligned} \frac{\partial \rho(x, y, t)}{\partial t} = & -\frac{\partial}{\partial x} \left\{ \left[C(x) + \sqrt{\frac{2Db}{a^2}}y \right] \rho(x, y, t) \right\} \\ & + \frac{\partial}{\partial y} \left[\frac{1}{\tau}y \rho(x, y, t) \right] + D' \frac{\partial^2}{\partial y^2} [\rho(x, y, t)] \end{aligned} \quad (6)$$

where $D' = \frac{D}{\tau^2}$, $\rho(x, y, t)$ is the PDF of the particle locating (x, y) at time t , parameters of a and b are the same to equation (2).

Owing to the non-autonomous item $\cos\left(\frac{\omega_0}{a}t + \varphi\right)$ $\rho(x, y, t)$, the equation (6) can't be solved by steady-state solution, and can't be solved by any exact solution [24].

We use the Taylor expansion, and derive the approximate periodic steady solution of equation (6) as below [24]

$$\begin{aligned} \rho(x|t) = & N_0 \sqrt{\frac{4\pi D^2 b}{a^2 \tau [1 - \tau c'(x, t)]}} \\ & \cdot \left\{ 1 + \frac{5Db\tau^3 [c''(x, t)]^2}{12a^2 [1 - \tau c'(x, t)]^5} \right\} \\ & \cdot \left\{ \left[\frac{\sqrt{2Db}}{a} - \frac{\tau \sqrt{2Db} c'(x, t)}{a} \right] \right\}^{\frac{3}{2}} \\ & \cdot \exp \left[\frac{1}{D} \int c(x, t) dx - \frac{1}{2D} \tau c^2(x, t) \right] \end{aligned} \quad (7)$$

where N_0 is the normalization constant,

$$c(x, t) = \begin{cases} x - x^3, & H_0 \\ x - x^3 \pm \sqrt{\frac{b}{a^3}}A \cos\left(\frac{\omega_0}{a}t + \varphi\right), & H_1 \end{cases}$$

is the drift force of the SR varying with the input signal, the parameters of a, b, τ and D is the same to equation (1) and (2).

B. THE PARTICLE'S PDF OF SR AT THE DECISION TIME

In order to apply the PDF of (7) to the detection and reception of sinusoidal wave, we assume that the SR processing of the electromagnetic particles is completed transiently, neglecting the transacting time from the unsteady state to the steady. That is the diffusion motion of the electromagnetic particles has already been periodic steady at the decision time. So

$$\begin{aligned} \rho(x|t_0) = & N_0 \sqrt{\frac{4\pi D^2 b}{a^2 \tau [1 - \tau c'(x, t_0)]}} \\ & \cdot \left\{ 1 + \frac{5Db\tau^3 [c''(x, t_0)]^2}{12a^2 [1 - \tau c'(x, t_0)]^5} \right\} \\ & \cdot \left\{ \left[\frac{\sqrt{2Db}}{a} - \frac{\tau \sqrt{2Db} c'(x, t_0)}{a} \right] \right\}^{\frac{3}{2}} \\ & \cdot \exp \left[\frac{1}{D} \int c(x, t_0) dx - \frac{1}{2D} \tau c^2(x, t_0) \right] \end{aligned} \quad (8)$$

where t_0 is the decision time, other parameters are the same as equation (1) (2) and (7).

As described in equation (8), the sinusoidal wave at decision time t_0 equals to the linear drift force pulling the particles to the bilateral well, which increase the pause probability at the bilateral well. The positive drift force pulls particles to the positive well, while the negative drift force pulls particles to the negative well. Therefore owing to the periodic sinusoidal wave and the symmetry of particles of SR, the output pdf of particles has symmetry properties. At the same time, different decision time decides different drift force because of the periodic properties of sinusoidal wave. The drift force reaches the largest when the decision time is the peak or valley of the sinusoidal wave, leading to that the pause time reaches the longest and the output pdf reaches the largest.

IV. THE QUADRATIC POLYNOMIAL RECEIVING SCHEME

A. THE TEST STATISTIC

So far, the test statistic in communication system mostly is the energy receiver, envelope receiver or matching filter receiver. All of them can be viewed as the generalized receiver of a quadratic polynomial structure. Base on this thought, we can set the $g(\bullet)$ be a quadratic polynomial item. And when the test statistic obeys the Gaussian distribution, the relationship of the error bit ratio P_e and the deflection d is analytical. What is more, the relationship of P_e and d is negatively correlated, when the test statistic obeys the non-Gaussian distribution. The d of non-Gaussian distribution can be defined as [8]

$$d^2 = \frac{(E[g(x)|H_1] - E[g(x)|H_0])^2}{\frac{1}{2}(\sigma[g(x)|H_1] + \sigma[g(x)|H_0])} \quad (9)$$

where $E[g(x)|H_1]$ and $\sigma[g(x)|H_1]$ are the expectation and standard deviation of $g(x)$ under the hypothesis H_1 , which are expressed as $E_1[g(x)]$ and $\sigma_1[g(x)]$ in the following; $E[g(x)|H_0]$ and $\sigma[g(x)|H_0]$ are the expectation and standard deviation of $g(x)$ under the hypothesis H_0 , which are expressed as $E_0[g(x)]$ and $\sigma_0[g(x)]$ in the following.

The parameters of $g(\bullet)$ can be determined by maximizing d , when $g(\bullet)$ is constrained by a quadratic polynomial. We assume that $g(x) = l_1x^2 + l_2x + l_3$, then the d of two hypothesis is (10), as shown at the bottom of this page.

As from the equation (10), the value of d of a quadratic polynomial is decided by the quadratic term l_1 , one degree term l_2 , and the one to four origin moment, dependent from the constant term l_3 . And d remains unchanged if we replace d by $\lambda d + \mu$, where λ and μ are arbitrary constants. Let $\mu_{11} = E_1[x]$, $\mu_{12} = E_1[x^2]$, $\mu_{13} = E_1[x^3]$, $\mu_{14} = E_1[x^4]$, $\mu_{01} = E_0[x]$, $\mu_{02} = E_0[x^2]$, $\mu_{03} = E_0[x^3]$ and $\mu_{04} = E_0[x^4]$, so the deflection, as (11), shown at the bottom of this page.

For simplification in the following, let

$$\begin{cases} c_{11} = (\mu_{12} - \mu_{02})^2 \\ c_{12} = 2(\mu_{12} - \mu_{02})(\mu_{11} - \mu_{01}) \\ c_{13} = (\mu_{11} - \mu_{01})^2 \\ c_{21} = (\mu_{14} - \mu_{12}^2 + \mu_{04} - \mu_{02}^2) \\ c_{22} = 2(\mu_{13} - \mu_{12}\mu_{11} + \mu_{03} - \mu_{02}\mu_{01}) \\ c_{23} = \mu_{12} - \mu_{11}^2 + \mu_{02} - \mu_{01}^2 \end{cases} \quad (12)$$

Let the equation (12) be substituted into the equation (11)

$$\frac{d^2(l_1, l_2)}{2} = \frac{l_1^2 c_{11} + l_1 l_2 c_{12} + l_2^2 c_{13}}{l_1^2 c_{21} + l_1 l_2 c_{22} + l_2^2 c_{23}} \quad (13)$$

Then the problem converts to

$$\max_{l_1, l_2 \in R} d(l_1, l_2) \quad (14)$$

For the necessary condition of extreme values of function, it can be

$$\begin{aligned} \frac{\partial d}{\partial l_1} = -\frac{\partial d}{\partial l_2} = 0 &\Leftrightarrow l_1^2(c_{11}c_{22} - c_{21}c_{12}) \\ &+ l_1 l_2(2c_{11}c_{23} - 2c_{21}c_{13}) \\ &+ l_2^2(c_{12}c_{23} - c_{13}c_{22}) = 0 \end{aligned} \quad (15)$$

Let $l_1 = ml_2$, then $\frac{\partial d}{\partial l_1} = 0$, so

$$\begin{aligned} \frac{\partial d}{\partial l_1} = 0 &\Leftrightarrow m^2(c_{11}c_{22} - c_{21}c_{12}) \\ &+ 2m(c_{11}c_{23} - c_{21}c_{13}) + (c_{12}c_{23} - c_{13}c_{22}) = 0 \end{aligned} \quad (16)$$

We can obtain the numerical solution of m by solving the equation (16). Then $g(x) = x^2 + \frac{1}{m}x + c$, and the mean and variance of $g(x)$ under two hypothesis are

$$\begin{cases} \mu_1 = E_1[g(x)] = \int g(x)\rho(x, t_0|H_1)dx \\ \mu_0 = E_0[g(x)] = \int g(x)\rho(x, t_0|H_0)dx \\ \sigma_1^2 = \sigma_1^2[g(x)] = \int (g(x) - \mu_1)^2 \rho(x, t_0|H_1)dx \\ \sigma_0^2 = \sigma_0^2[g(x)] = \int (g(x) - \mu_0)^2 \rho(x, t_0|H_0)dx \end{cases} \quad (17)$$

$$\begin{aligned} d^2(l_1, l_2, l_3) &= \frac{(E_1[g(x)] - E_0[g(x)])^2}{\frac{1}{2}(\sigma_1[g(x)] + \sigma_0[g(x)])} \\ &= \frac{(l_1 E_1[x^2] + l_2 E_1[x] - l_1 E_0[x^2] - l_2 E_0[x])^2}{\frac{1}{2}(l_1^2 \sigma_1[x^2] + l_2^2 \sigma_1[x] - l_1^2 \sigma_0[x^2] - l_2^2 \sigma_0[x])} \\ &= \frac{[l_1(E_1[x^2] - E_0[x^2]) + l_2(E_1[x] - E_0[x])]^2}{\frac{1}{2} \left[l_1^2 E_1[x^4] + 2l_1 l_2 E_1[x^3] + l_2^2 E_1[x^2] - (l_1^2 E_1^2[x^2] + 2l_1 l_2 E_1[x^2] E_1[x] + l_2^2 E_1^2[x]) \right]} \\ &= \frac{[l_1(E_1[x^2] - E_0[x^2]) + l_2(E_1[x] - E_0[x])]^2}{\frac{1}{2} \left[l_1^2 E_0[x^4] + 2l_1 l_2 E_0[x^3] + l_2^2 E_0[x^2] - (l_1^2 E_0^2[x^2] + 2l_1 l_2 E_0[x^2] E_0[x] + l_2^2 E_0^2[x]) \right]} \\ &= d^2(l_1, l_2) \end{aligned} \quad (10)$$

$$d^2(l_1, l_2) = \frac{l_1^2(\mu_{12} - \mu_{02})^2 + 2l_1 l_2(\mu_{12} - \mu_{02})(\mu_{11} - \mu_{01}) + l_2^2(\mu_{11} - \mu_{01})^2}{\frac{1}{2} \left[l_1^2(\mu_{14} - \mu_{12}^2 + \mu_{04} - \mu_{02}^2) + 2l_1 l_2(\mu_{13} - \mu_{12}\mu_{11} + \mu_{03} - \mu_{02}\mu_{01}) + l_2^2(\mu_{12} - \mu_{11}^2 + \mu_{02} - \mu_{01}^2) \right]} \quad (11)$$

Processed by the unite of $\frac{1}{N} \sum$, the average of N numbers of $g(x_0)$ with the same expectation and variance is obtained. And the $g(x_0)$ are independent and identically distributed random variables at different t_0 . What is more, the central limit theorem is that the average of N numbers of independent and identically distributed random variables with the same expectation and variance obeys the Gaussian distribution when N is above 50 [25]. And the $g(x_0)$ is the independent and identically distributed random variables with the same expectation and variance. And the test statistic is the average of N numbers of $g(x_0)$. So it obeys the Gaussian distribution

$$\Lambda(t_0) = \frac{1}{N} \sum g(x_0) \sim \begin{cases} N(\mu_1, \sigma_1^2/N), & H_1 \\ N(\mu_0, \sigma_0^2/N), & H_0 \end{cases} \quad (18)$$

where μ_1 and σ_1 are the expectation and variance of $g(x_0)$ under the hypothesis of H_1 . while μ_0 and σ_0 are the expectation and variance of $g(x_0)$ under the hypothesis of H_0 .

Till then, the quadratic polynomial reception of sinusoidal signal enhanced by SR has been converted to the hypothesis testing problem under Gaussian distribution.

What is more, the frequency of the sinusoidal wave is known priory at the receiving end. The receiving symbol is decided as “1”, when the sinusoidal signal is been detected. Otherwise the receiving symbol is decided as “0”. Base on the criterion of minimum error probability, the bit error ratio (BER)

$$\begin{aligned} P_e &= \frac{1}{2} (1 - P_d) + \frac{1}{2} P_{fa} \\ &= \frac{1}{2} \left[\int_{-\infty}^{r_0} f_1(\Lambda) d\Lambda + \int_{r_0}^{+\infty} f_0(\Lambda) d\Lambda \right] \\ &= \frac{1}{2} - \frac{1}{2} Q \left(\frac{r_0 - \mu_1}{\sqrt{\sigma_1^2/N}} \right) + \frac{1}{2} Q \left(\frac{r_0 - \mu_0}{\sqrt{\sigma_0^2/N}} \right) \end{aligned} \quad (19)$$

where r_0 is the threshold, μ_1, σ_1, μ_0 and σ_0 are the same as equation (18).

As for likelihood ratio detection, the P_e reaches the minimum when the value of the PDF of two hypothesis is equal like $f_1(r_0) = f_0(r_0)$, that is

$$\frac{1}{\sqrt{2\pi\sigma_1^2/N}} e^{-\frac{(r_0-\mu_1)^2}{2\sigma_1^2/N}} = \frac{1}{\sqrt{2\pi\sigma_0^2/N}} e^{-\frac{(r_0-\mu_0)^2}{2\sigma_0^2/N}} \quad (20)$$

Simplified as

$$\frac{(r_0 - \mu_1)^2}{\sigma_1^2} - \frac{(r_0 - \mu_0)^2}{\sigma_0^2} = \frac{2}{N} \ln \frac{\sigma_1}{\sigma_0} \quad (21)$$

Then the threshold r_0 can be numerically calculated by equation (21).

B. THE RECEIVING ALGORITHM FLOW

Base on the theory of 4.1, the receiving algorithm flow of the sinusoidal signal enhanced by SR can be concluded as follows:

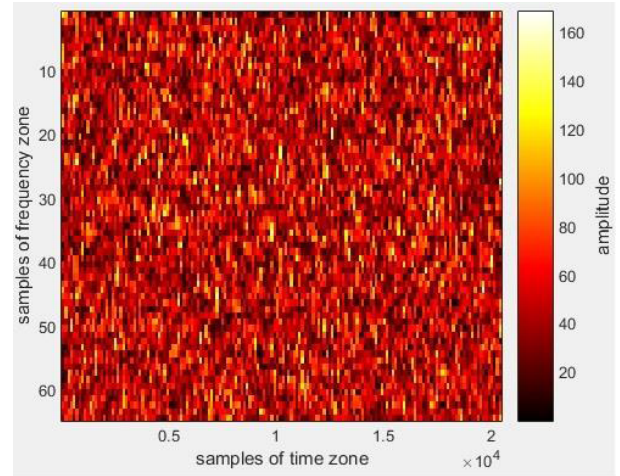


FIGURE 2. The time-frequency waveform of the RF signal of DSFH (SNR = -20dB).

- 1) Calculate the SR output PDF $\rho(x, t|H_1)$ and $\rho(x, t|H_0)$ of the two hypothesis, and the one to four origin moment $\mu_{11}, \mu_{12}, \mu_{13}, \mu_{14}$ and $\mu_{01}, \mu_{02}, \mu_{03}, \mu_{04}$, based on the equation (8);
- 2) Calculate the coefficients l_1 and l_2 , based on the equation (12) (13) (15) and (16);
- 3) Calculate the expectation μ_1, μ_0 and variance σ_1, σ_0 of $g(x)$ under two hypothesis based on equation (17);
- 4) Calculate the threshold r_0 of the criterion of minimum error probability, based on equation (21);
- 5) Calculate the P_e based on the equation (19).

V. SIMULATION RESULTS AND DISCUSSIONS

In this section, the theory and simulation are analyzed to demonstrate the detection improvement by the Simulink model of the IF signal via SR processing. And in our case, the IF signal is received by super-heterodyne receiver in DSFH. For visual impression, the radio frequency (RF) signal of DSFH at very low SNR is also simulated by Simulink model. The simulation parameters are as follows: the frequency of the IF signal is 1 kHz; the sample frequency of IF signal is 200 kHz; the frequency hopping section is 30-88 kHz; the sample frequency of RF signal is 2000 kHz.

A. TIME AND FREQUENCY FEATURE ANALYSIS OF THE RF SIGNAL OF DSFH

The time-frequency graph of the RF signal of the DSFH is described as Fig. 2. The time samples, the frequency samples and the amplitude are abscissa, ordinate and stroke coordinates respectively. Owing to that the sample frequency is 2000 kHz and that the hamming window length is 128, the hopping frequency spots concentrate on the upside of the positive frequency band of 1000 kHz. The time-frequency graph is filled with dark noise spots in Fig. 2. This is because that the signal is submerged in the strong noise when input SNR is -20 dB. So time-frequency graph is fully filled by

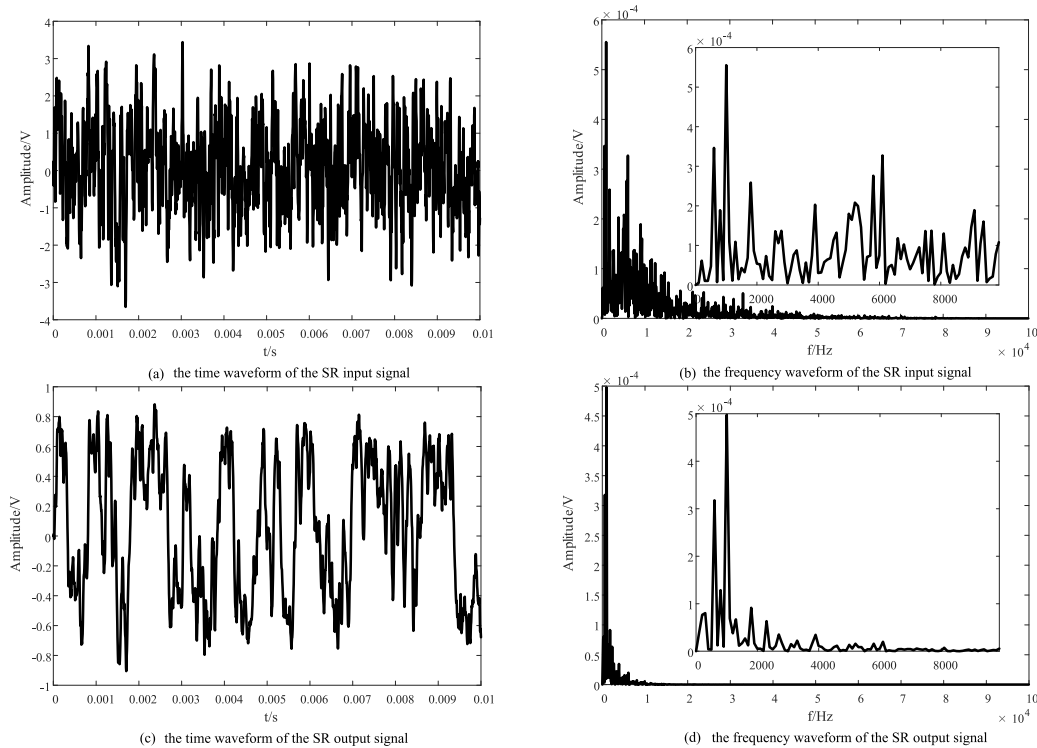


FIGURE 3. The time and frequency waveform of the IF signal of the DSFH via SR processing (SNR = -18dB, $\sigma^2 = 4, A = 0.25, a = 1 \times 10^4, b = 2.59 \times 10^{12}$).

noise spots. That is why the traditional FH can not work well in the strong noise.

B. TIME AND FREQUENCY WAVEFORM OF THE IF SIGNAL PROCESSED BY SR

The time and frequency waveform of the IF signal submerged in strong noise is shown in Fig. 3(a) and (b). At the same time, the time and frequency waveform of the SR output signal is shown in Fig. 3(c) and (d). It presents cluttered and irregularities, and there is no character of the sinusoidal wave of 1 kHz when SNR is -18 dB in Fig. 3(a) and (b). However periodic features can be found in the time waveform of Fig. 3(c), and the signal component of 1 kHz (samples are 20000, and frequency resolution is 10Hz) can be observed significantly in the frequency waveform of Fig. 3(d). More importantly, the SNR is increased by 8.5521 dB and the output SNR is -9.4479 dB. This is because the color noise is concentrated in the low frequency region resulting in an increase in the energy of this region, which pulls the particles to resonate between two wells together with the sinusoidal wave. This is equivalent to a nonlinear low-pass filter which only allows the low frequencies to pass. Therefore the signal exhibits a degree of periodicity in the time zone, apparently in the frequency zone where the SNR increases in macroscopic view.

C. THE PDF OF THE IF SIGNAL PROCESSED BY SR

The theoretical and simulation results of the PDF of the IF signal processed by SR are described in Fig. 4(a) and (b).

It is the color noise filtered by transition bands in Fig. 4(a), and filtered by pass band in Fig. 4(b). The force of sinusoidal wave can pull the particles to center at the both sides of wells, leading to expand the difference of the hypotheses of H_1 and H_0 , which is useful to distinguish the existence of the sinusoidal wave of the hypotheses of H_1 and H_0 . And the difference of the PDF under H_1 and H_0 is more obvious in Fig. 4(a) than in Fig. 4(b). This is because that the color noise mostly distributes on the band of $(-\frac{\pi}{\tau}, \frac{\pi}{\tau})$. When $\tau = 0.0035$, the IF signal of 1 kHz locates in the transitional zone. While $\tau = 0.1$, the IF signal of 1 kHz locates in the pass-band zone. So the intensity of the color noise filtered by transition bands is lower than the color noise filtered by pass bands, leading to that the local SNR is larger.

D. THE BER OF DIFFERENT CORRELATION TIME OF COLOR NOISE OF QUADRATIC POLYNOMIAL RECEIVER

The theoretical and simulation results of the BER of different receiver are described in Fig. 5. We can see that the smaller the color noise correlation time of the quadratic polynomial receiver, the smaller the BER. This is because that the color noise is mainly distributed in the frequency band of $(-\frac{\pi}{\tau}, \frac{\pi}{\tau})$. We use the color noise to describe the noise filtered by low-pass filter. And when the noise intensity is constant, the smaller the correlation time, and the color noise is more concentrated due to the better performance of the low-pass filter. Moreover, when $\tau = 0.0035$, the band of the color noise is almost (-1kHz, 1kHz), the edge of the IF signal is located there on. And the bigger the τ , the wider the band of

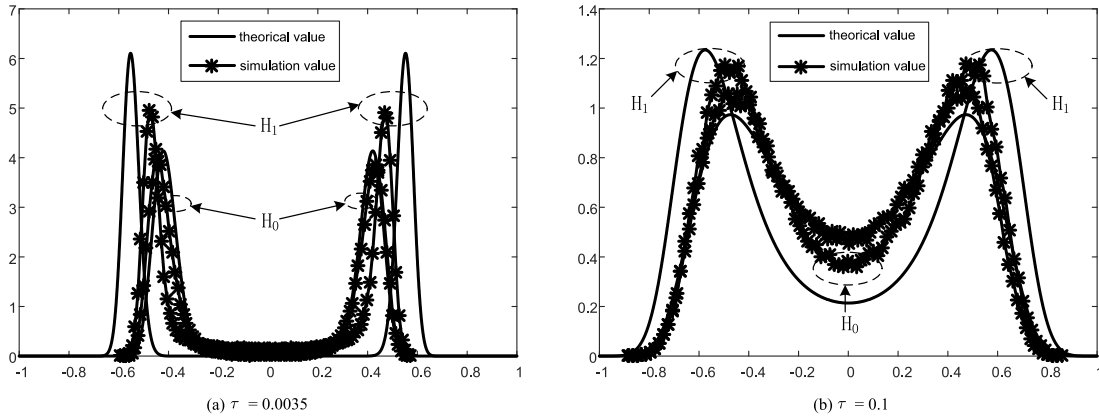


FIGURE 4. PDF of the particles at different position (SNR = -14dB, $\sigma^2 = 4$, $A = 0.4$, $a = 1 \times 10^4$, $b = 5.65 \times 10^{12}$).

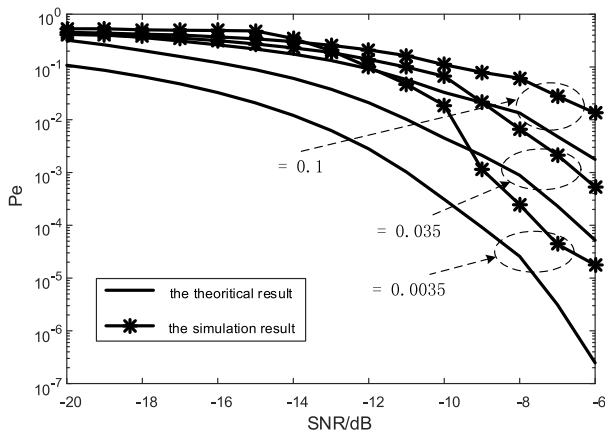


FIGURE 5. The BER of the quadratic polynomial receiver of different correlation time of color noise ($N = 10$).

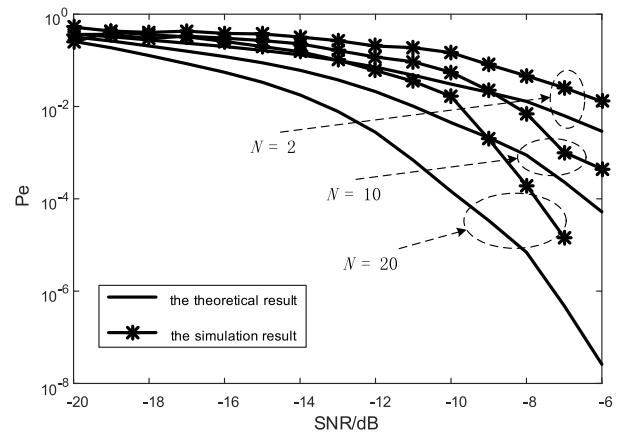


FIGURE 7. The BER of different N of the quadratic polynomial receiver ($\tau = 0.035$).

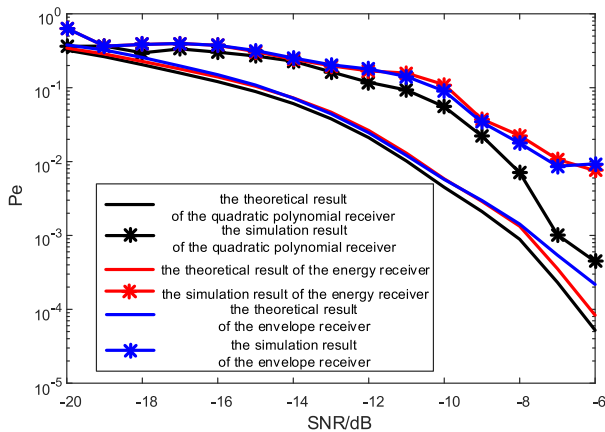


FIGURE 6. The BER of different receivers ($N = 10$, $\tau = 0.035$).

the color noise, whose band the IF signal locates in. So the local SNR of $\tau = 0.0035$ is biggest of the experiment. That is why the BER of the $\tau = 0.0035$ is the smallest.

E. THE BER OF DIFFERENT RECEIVERS

The theoretical and simulation results of the BER of different receivers are described in Fig. 6. It can be seen that the

BER of the quadratic polynomial receiver is the smallest of the three receivers, then is the energy receiver and last is the envelope receiver which are verified by theory and simulation. That is because that the one degree term l_2 brings some receiving gain of the quadratic polynomial receiver contrast to the energy receiver, at the same time, the energy receiver is almost the same to the envelope receiver due to that they are all based on energy detection. And the deflection of the quadratic polynomial receiver is the biggest of the three receivers leading to smallest error bit. But the difference is small because that the one degree term is [0.0019, 0, 0, -0.1198, -0.0296, 0.0319, -0.0590, -0.425, -0.0544, -0.0156, 0.0161, -0.0180, 0.0163, -0.0192, -0.0249], little different from the quadratic term of 1. So we can conclude that the quadratic polynomial term of receiving of the sinusoidal signal enhanced by SR plays a major role, while the one degree term plays a minor role.

F. THE BER OF DIFFERENT N OF THE QUADRATIC POLYNOMIAL RECEIVER

The theoretical and simulation results of the BER of different N of the quadratic polynomial receiver are described in Fig. 7. We can see that the bigger the N , the smaller the

error bit ratio, verified by theoretical and simulation results. This is because that when the receiver is certain, different N just affects the variance of the test statistics. And the variance decreases following the increase of N . The smaller the variance, the bigger the separation of two hypothesis, leading to better receiving performance. But with the increase of N , it needs more period of sinusoidal wave during one symbol time to decide. So when the system sample frequency and the frequency of IF signal are certain, the sending rate of symbols must be decreased. This is also the thought of “the efficiency replaces the reliability”. Ignoring the difference of two hypothesis and assuming the binary symmetric channels, the relationship between the maximum of information rate c of single symbol and the error bit P_e is $c = 1 + P_e \log_2(P_e) + (1 - P_e) \log_2(1 - P_e)$. So the relationship between the maximum of symbol rate R and the error bit P_e is $R = \frac{f_0}{N}c = \frac{f_0}{N} [1 + P_e \log_2(P_e) + (1 - P_e) \log_2(1 - P_e)]$. when $N = 20$, and the SNR is above -14 dB, the error bit of the quadratic polynomial receiver is less than 1×10^{-2} . At the same time, the symbol rate is 50 bps, with the sample frequency is 200 kHz and the IF frequency is 1 kHz. So we can apply it to the military emergency communication like submarine communication.

Noting: for the computing restriction of simulation, we do not get the P_e less than 10^{-6} further, but the tendency of simulation and theoretical results is already obvious.

G. AN APPLICATION EXAMPLE OF THE RECEIVING SCHEME

At the beginning of using DSFH [1], [2], the current communication circumstances should be detected and estimated. Therefore, we can obtain the range of SNR and the correlation time of color noise which is the initial condition. Next we give an example of how to apply the receiving scheme in DSFH system.

1) The initial condition of applying the receiving scheme

Assume that the SNR = -10 dB, $\tau = 0.035$ in the communication circumstances. And the IF frequency and sample frequency of the super-heterodyne receiver of DSFH is 1 kHz and 200 kHz.

2) The process of applying the receiving scheme

① By using the step of 1 to 3 of “the receiving algorithm flow”, we obtain the quadratic polynomial receiving structure $g(x) = x^2 + 0.0161x$;

② Using the step of 4 and 5 of “the receiving algorithm flow”, we can calculate three results e.g. $P_e = 0.030630, N = 2, P_e = 0.004492, N = 10$ and $P_e = 0.000146, N = 20$;

③ Using the $R = \frac{f_0}{N}c = \frac{f_0}{N} [1 + P_e \log_2(P_e) + (1 - P_e) \log_2(1 - P_e)]$, we get three results e.g. $P_e = 0.030630, R = 401\text{bit}; N = 2, P_e = 0.004492, R = 96\text{bit}; N = 10$ and $P_e = 0.000146, R = 50\text{bit}; N = 20$.

④ For further expanding the application of “the receiving algorithm flow”, we obtain the P_e and R when SNR = $-12, -11, -9, -8, -7, -6$ dB; $\tau = 0.035$ as in Fig. 8.

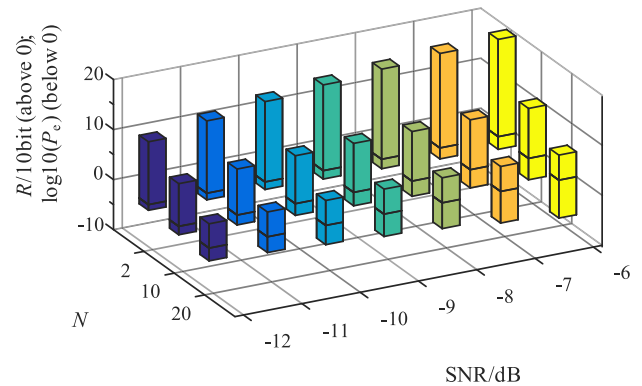


FIGURE 8. The BER and symbol rate of different N of the quadratic polynomial receiver ($\tau = 0.035$).

The SNR and N are the abscissa and ordinate coordinates respectively, however $R/10$ is above 0 and $\log_{10}(P_e)$ is below 0 in stroke coordinates for better comparison. We can see that the for better P_e , we must increase N leading decreasing R at a certain communication condition(a certain SNR and τ). And the P_e representing the reliability and R representing the efficiency keep a balance.

3) The suggestion of applying the receiving scheme

When the communication circumstance is certain, and the super-heterodyne receiver of DSFH is fixed, we can pursue better R or better P_e by changing N of using the quadratic polynomial receiving structure. For better P_e , we must decrease R by increasing N .

VI. CONCLUSIONS

The SR system has the natural resonated effect for the small frequency signal when the input signal, the noise and the parameters of SR are matched. The IF signal received by the super-heterodyne receiver can become equivalent to a low frequency signal by means of over-sampling. Thus, using SR, the noise together with the low frequency signal can be enhanced in the low frequency zone. And the color noise can further enhance the SR. By analyzing the SR mechanism of sinusoidal signals under color noise and assuming the SR transitive motion of electronic particles to be instant, we introduce the decision time. As the focus of the test statistics at decision time only, the non-autonomous FPE is transacted to an autonomous one. Next, the periodic steady-state solution of FPE with the decision time parameter is obtained. A quadratic polynomial receiving scheme for sinusoidal signals enhanced by SR under color noise is proposed and compared with the energy and the matched filtering receivers. We conclude that: 1) when the intensity of the noise is constant, the smaller the correlation time, the bigger the local SNR around the IF frequency due to the better performance of the low-pass filter; 2) The error bit of the quadratic polynomial receiver is less than 1×10^{-2} when $N = 20$ and the SNR is above -14 dB. At the same time, the symbol rate is 50bps, with the sample frequency

is 200 kHz and the IF frequency is 1 kHz. So we can apply the proposed scheme to the cases that instantaneous receiving signal is sinusoidal of the most super-heterodyne receiver in military emergency communication under extremely low SNR, e.g. DSFH and submarine communication. The idea of “determine the decision time first, and then determine the test statistics” can be utilized for signal reception by SR enhancement. What is more, the quadratic polynomial receiving scheme is better than energy receiving and envelope receiving schemes in sinusoidal signals receiving enhanced by SR. And the parameters of the receiving scheme can be calculated by the proposed algorithm. And the proposed receiving scheme can be applied to other cases under low SNR.

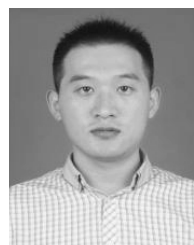
REFERENCES

- [1] G. Liu, Y. Kang, H. Quan, H. Sun, P. Cui, and C. Guo, “The detection performance of the Dual-Sequence-Frequency-Hopping signal via stochastic resonance processing under color noise,” *Radioengineering*, vol. 27, no. 3, pp. 618–626, Sep. 2019, doi: [10.13164/re.2019.0618](https://doi.org/10.13164/re.2019.0618).
- [2] G. K. Liu, H. D. Quan, Y. M. Kang, H. X. Sun, P. Z. Cui, and Y. M. Han, “A quadratic polynomial receiving scheme for sine signals enhanced by stochastic resonance,” *Acta Phys. Sinica*, vol. 68, no. 21, 2019, Art. no. 210501, doi: [10.7498/aps.68.20190952](https://doi.org/10.7498/aps.68.20190952).
- [3] G. K. Liu, H. D. Quan, H. X. Sun, P. Z. Cui, K. Chi, and S. L. Yao, “Stochastic resonance detection method for the dual-sequence frequency hopping signal under extremely low signal-to-noise ratio,” *J. Electron. Inf. Technol.*, vol. 41, no. 10, pp. 2342–2349, 2019, doi: [10.11999/JEIT190157](https://doi.org/10.11999/JEIT190157).
- [4] L. Li, L. Sboui, Z. Rezki, and M.-S. Alouini, “On the capacity of fading channels with peak and average power constraints at low SNR,” *IEEE Trans. Veh. Technol.*, vol. 68, no. 1, pp. 93–100, Jan. 2019, doi: [10.1109/TVT.2018.2882684](https://doi.org/10.1109/TVT.2018.2882684).
- [5] R. Benzi, A. Sutera, and A. Vulpiani, “The mechanism of stochastic resonance,” *J. Phys. A, Math. Gen.*, vol. 14, no. 11, pp. 453–457, Nov. 1981.
- [6] L. Gammaitoni, P. Hänggi, and P. Jung, “Stochastic resonance,” *Rev. modern Phys.*, vol. 70, no. 1, pp. 223–287, 1998.
- [7] J. Liu, J. Mao, B. Huang, and P. Liu, “Chaos and reverse transitions in stochastic resonance,” *Phys. Lett. A*, vol. 382, nos. 42–43, pp. 3071–3078, Oct. 2018, doi: [10.1016/j.physleta.2018.08.016](https://doi.org/10.1016/j.physleta.2018.08.016).
- [8] J. Tougaard, “Signal detection theory, detectability and stochastic resonance effects,” *Biol. Cybern.*, vol. 87, no. 2, pp. 79–90, Aug. 2002, doi: [10.1007/s00422-002-0327-0](https://doi.org/10.1007/s00422-002-0327-0).
- [9] Y.-M. Kang, “Simulating transient dynamics of the time-dependent time fractional Fokker–Planck systems,” *Phys. Lett. A*, vol. 380, no. 39, pp. 3160–3166, Sep. 2016, doi: [10.1016/j.physleta.2016.07.049](https://doi.org/10.1016/j.physleta.2016.07.049).
- [10] S. Wang and F. Wang, “Adaptive stochastic resonance system in terahertz radar signal detection,” *Acta Phys. Sci.*, vol. 67, no. 16, pp. 249–255, 2018, doi: [10.7498/aps.67.20172367](https://doi.org/10.7498/aps.67.20172367).
- [11] P. Krauss, C. Metzner, A. Schilling, C. Schätz, K. Tziridis, B. Fabry, and H. Schulze, “Adaptive stochastic resonance for unknown and variable input signals,” *Sci. Rep.*, vol. 7, no. 1, pp. 2450–2456, Dec. 2017, doi: [10.1038/s41598-017-02644-w](https://doi.org/10.1038/s41598-017-02644-w).
- [12] G. Zhang, D. Hu, and T. Zhang, “Stochastic resonance in unsaturated piecewise nonlinear bistable system under multiplicative and additive noise for bearing fault diagnosis,” *IEEE Access*, vol. 7, pp. 58435–58448, 2019, doi: [10.1109/ACCESS.2019.2914138](https://doi.org/10.1109/ACCESS.2019.2914138).
- [13] V. Galdi, V. Pierro, and I. M. Pinto, “Evaluation of stochastic-resonance-based detectors of weak harmonic signals in additive white Gaussian noise,” *Phys. Rev. E, Stat. Phys. Plasmas Fluids Relat. Interdiscip. Top.*, vol. 57, no. 6, pp. 6470–6479, Jun. 1998, doi: [10.1103/PhysRevE.57.6470](https://doi.org/10.1103/PhysRevE.57.6470).
- [14] M. A. Fuentes, H. S. Wio, and T. Raúl, “Effective Markovian approximation for non-Gaussian noises: A path integral approach,” *Phys. A, Stat. Mech. Appl.*, vol. 303, no. 1, pp. 91–104, 2002, doi: [10.1016/S0378-4371\(01\)00435-6](https://doi.org/10.1016/S0378-4371(01)00435-6).
- [15] H. Chen, P. K. Varshney, S. M. Kay, and J. H. Michels, “Theory of the stochastic resonance effect in signal detection: Part I—Fixed detectors,” *IEEE Trans. Signal Process.*, vol. 55, no. 7, pp. 3172–3184, Jul. 2007, doi: [10.1109/TSP.2007.893757](https://doi.org/10.1109/TSP.2007.893757).
- [16] H. Chen and P. K. Varshney, “Theory of the stochastic resonance effect in signal Detection—Part II: Variable detectors,” *IEEE Trans. Signal Process.*, vol. 56, no. 10, pp. 5031–5041, Oct. 2008, doi: [10.1109/TSP.2008.928509](https://doi.org/10.1109/TSP.2008.928509).
- [17] R. N. Liu, Y. M. Kang, and Y. X. Fu, “Stochastic resonance and bifurcation of order parameter in a coupled system of underdamped duffing oscillators,” *Int. J. Bifurcation Chaos*, vol. 29, no. 8, p. 1950108, 2019, doi: [10.1142/S0218127419501086](https://doi.org/10.1142/S0218127419501086).
- [18] L. Zhang and A. Song, “Realizing reliable logical stochastic resonance under colored noise by adding periodic force,” *Phys. A, Stat. Mech. Appl.*, vol. 503, pp. 958–968, Aug. 2018, doi: [10.1016/j.physa.2018.08.062](https://doi.org/10.1016/j.physa.2018.08.062).
- [19] T. Xia, Y. Song, Y. Zheng, E. Pan, and L. Xi, “An ensemble framework based on convolutional bi-directional LSTM with multiple time windows for remaining useful life estimation,” *Comput. Ind.*, vol. 115, Feb. 2020, Art. no. 103182, doi: [10.1016/j.compind.2019.103182](https://doi.org/10.1016/j.compind.2019.103182).
- [20] T. Xia, Y. Dong, L. Xiao, S. Du, E. Pan, and L. Xi, “Recent advances in prognostics and health management for advanced manufacturing paradigms,” *Rel. Eng. Syst. Saf.*, vol. 178, pp. 255–268, Oct. 2018, doi: [10.1016/j.res.2018.06.021](https://doi.org/10.1016/j.res.2018.06.021).
- [21] F. Duan, L. Duan, F. Chapeau-Blondeau, Y. Ren, and D. Abbott, “Binary signal transmission in nonlinear sensors: Stochastic resonance and human hand balance,” *IEEE Instrum. Meas. Mag.*, vol. 23, no. 1, pp. 44–49, Feb. 2020, doi: [10.1109/MIM.2020.8979523](https://doi.org/10.1109/MIM.2020.8979523).
- [22] X. Liu, H. Wang, Y. Meng, and M. Fu, “Classification of hyperspectral image by CNN based on shadow area enhancement through dynamic stochastic resonance,” *IEEE Access*, vol. 7, pp. 134862–134870, 2019, doi: [10.1109/ACCESS.2019.2941872](https://doi.org/10.1109/ACCESS.2019.2941872).
- [23] N. Q. HU, *Theory and Method of Detecting Weak Characteristic Signals of Stochastic Resonance*. Beijing, China: National Defense Industry Press, 2012, pp. 85–86.
- [24] G. HU, *Stochastic Forces and Nonlinear Systems*. Shanghai, China: Shanghai Scientific and Technological Education, 1994, pp. 222–232.
- [25] Z. Sheng, S. Q. Xie, and C. Y. Pan, *The Probability Theory and Mathematical Statics*. Beijing, China: Higher Education Press, 2008, pp. 147–153.



emphasis on signal processing in communications.

HOUDE QUAN was born in Dalian, China, in 1957. He received the M.E. degree in radar engineering from the Mechanical Engineering College, Shijiazhuang, China, in 1983, and the Ph.D. degree in communications and information systems from Northwestern Polytechnical University, Xian, China, in 2003. He is currently with Army Engineering University, Shijiazhuang, as a Professor. His research interests include spread spectrum communications and wireless mobile systems with



GUANGKAI LIU was born in Shijiazhuang, China, in 1990. He received the M.E. degree in control engineering from the Mechanical Engineering College, Shijiazhuang, in 2015. He is currently pursuing the Ph.D. degree with Army Engineering University, Shijiazhuang. His research interests include weak signal detection and stochastic resonance.

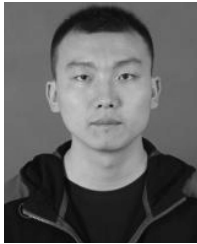


HUIXIAN SUN was born in Linhe, China, in 1980. He received the Ph.D. degree in instrument science and technology from the National University of Defense Technology, Changsha, China, in 2010. He is currently with Army Engineering University, Shijiazhuang, China, as a Lecturer. His research interests include command information system engineering and tactical wireless communications technology.



XIAOLU ZHANG was born in Shijiazhuang, China, in 1993. She received the B.E. degree in control engineering from the Mechanical Engineering College, Shijiazhuang, in 2015. She is currently pursuing the M.E. degree with Army Engineering University, Shijiazhuang. She is also an Engineer of the troop of 95010. Her research interests include weak signal detection and stochastic resonance.

...



XIAOHAN WANG was born in Hengshui, China, in 1992. He received the M.E. degree in control engineering from the Mechanical Engineering College, Shijiazhuang, China, in 2015. He is currently pursuing the Ph.D. degree with Army Engineering University, Shijiazhuang. His research interest includes information security.